Low temperature exchange bias in [$DyFe_2$/YFe_2] superlattices: effect of the thermo-magnetic preparation

2009 J. Phys.: Condens. Matter 21 236002

(http://iopscience.iop.org/0953-8984/21/23/236002)

J. Phys.: Condens. Matter **21** (2009) 236002 (7pp) doi:10.1088/0953-8984/21/23/236002

Low temperature exchange bias in [$DyFe_2/YFe_2$] superlattices: effect of the thermo-magnetic preparation

K Dumesnil[1,3], C Dufour[1], S Fernandez[1], M Oudich[1], A Avisou[1], A Rogalev[2] and F Wilhelm[2]

[1] Laboratoire de Physique des Matériaux (UMR CNRS 7556), Université H Poincaré-Nancy I, BP 239, 54506 Vandoeuvre les Nancy cedex, France
[2] European Synchrotron Radiation Facility, BP 220, 38043 Grenoble cedex, France

E-mail: dumesnil@lpm.u-nancy.fr

Received 2 March 2009, in final form 7 April 2009
Published 7 May 2009
Online at stacks.iop.org/JPhysCM/21/236002

Abstract
The effect of the thermo-magnetic preparation on exchange bias is investigated in an exchange-coupled [3 nm $DyFe_2$/12 nmYFe_2]$_{22}$ superlattice. X-ray magnetic circular dichroism (XMCD) experiments at low temperature reveal that exchange bias originates from the quenched $DyFe_2$ magnetization, biasing the unpinned YFe_2 reversal. This quenched configuration can be tailored by changing the cooling field or the magnetic preparation at 300 K before zero-field cooling. Changing the amplitude of the cooling field induces interface domain walls and tends to modify the orientation of the pinning moments at the interfaces. This results in the observation of single loops and in the continuous variation of the bias field as a function of the cooling field. A specific magnetic preparation (field cycling) at 300 K induces different remanent states with lateral domains in the pinning layer, which remain unchanged at low temperature after zero-field cooling and behave independently. This gives rise to combined loops, whose shape reflects the domain populations.

1. Introduction

Exchange-coupled systems combine two different magnetic materials that magnetically interact with each other at their interfaces via the exchange coupling mechanism. This interaction tends to strongly modify the magnetic behavior of each material compared to their individual properties, as for example the coercivity and the anisotropy. Moreover, the interface exchange coupling is at the origin of interesting phenomena that have been generating intense research activities for several years: the spring magnet behavior [1] and the exchange bias effect [2, 3].

Traditionally, exchange bias is defined in ferromagnet (FM)/antiferromagnet (AF) systems as the shift of the FM magnetization about the zero of applied field [4]. Exchange bias is often observed when unpinned spins of a FM are coupled to pinned spins of an AF that produce a unidirectional magnetic anisotropy [2, 3]. Precise understanding of exchange bias thus requires a good knowledge of the spin structure in the AF, especially close to the interfaces [5, 6]. Pinned magnetization is, however, typically a per cent or so of the saturation magnetization, and thus, challenging to detect and quantify. The use of element-selective and highly sensitive x-ray techniques, such as x-ray magnetic circular dichroïsm (XMCD), and/or spatially resolved approaches, such as polarized neutron reflectometry, are often required to derive information on the subtle interface magnetic structure and to correlate this to exchange bias properties [7–14].

The study of alternative exchange-coupled systems combining hard/soft ferromagnetic or ferrimagnetic materials is interesting, given the possibility to address more easily specific issues concerning the pinning of the magnetically hard layer. Provided that the external field does not exceed its coercivity, the hard material can play the role of the AF in inhibiting the soft magnetization reversal. Moreover, (hard/soft) and (FM/AF) systems both exhibit

[3] Address for correspondence: Laboratoire de Physique des Matériaux (UMR 7556), Université Henri Poincaré-Nancy I, BP 239, 54506 Vandoeuvre les Nancy cedex, France.

pinned magnetization and interface domain walls (IDW) developing parallel to the unpinned/pinned interfaces, which makes the comparison of their exchange bias properties relevant.

Among the systems studied in this field, the $REFe_2$ (RE = rare earth) Laves phase superlattices are of interest for potential applications [15, 16]. They are also among the few single crystalline superlattices that exhibit spring magnet behavior [17–19], most of the other systems being either textured polycrystalline [20, 21] or amorphous [22] materials, or consisting of randomly oriented magnetically hard grains embedded in a soft matrix [23]. $DyFe_2$ is a hard ferrimagnet with a resultant magnetization (4.6 μ_B/f.u. at 300 K) along the dominant Dy subnet magnetization. YFe_2 is a soft ferrimagnet, but as the yttrium site only has a small induced moment [24], the iron contribution is the dominant one (2.79 μ_B/f.u. at 300 K). Due to the strong exchange interaction between iron moments, the magnetic coupling at the $DyFe_2/YFe_2$ interfaces occurs mainly through the ferromagnetic coupling between iron spins, which results in a global antiparallel coupling between the net magnetizations of the $DyFe_2$ and YFe_2 layers [25].

Such an AF exchange interaction across the interface usually yields a positive exchange bias field for strong cooling fields, while the exchange bias is negative in the majority of systems [2, 3]. The exchange bias is directly related to the interface pinned configuration in the AF or hard layer that may be sensitive to the thermo-magnetic preparation of the system. In the case of AF interface exchange interaction, the bias field exhibits large changes as a function of cooling field [26–28]. Moreover, it has been shown recently that the occurrence of large lateral domains with opposite spin orientations in the AF or hard layer may lead to the observation of bifurcated hysteresis loops, shifted in opposite directions [29, 30].

In this paper, we report on the strong bias effect observed at low temperature in a [3 nm $DyFe_2$/12 nm YFe_2]$_{22}$ superlattice. The aim is to address the influence of the magnetic preparation on the bias field. It consequently focuses on the *low temperature* behavior, where the exchange bias field is the largest. In this hard/soft system the exchange bias is related to the pinned magnetic configurations in the hard layers; it is thus observed in the temperature range where the $DyFe_2$ magnetization remains frozen when applying an external magnetic field. However, when increasing temperature above 100 K, the bias effect vanishes because the magnetization reversal process of the whole superlattice drastically changes and evolves towards a regime where the hard $DyFe_2$ layers reverse first [31].

For this study, x-ray magnetic circular dichroïsm (XMCD) experiments are combined with magnetometry measurements to separately analyze the magnetic behavior of the two materials constituting the system. This permits us to correlate the observed exchange bias to the different magnetic configurations imprinted in the hard $DyFe_2$ layers. Two types of magnetic preparations are investigated (i) cooling the sample in an applied field of various magnitudes (ii) cooling the sample in zero magnetic field, after a specific field cycling at room temperature which leads to different remanent states. By choosing the appropriate conditions, the magnetic configuration in $DyFe_2$ can be controlled to tailor specific exchange bias.

2. Experimental details

The superlattice has been grown by molecular beam epitaxy following the growth process originally developed in our group for the epitaxial growth of $REFe_2$ thin films [32]: a $(11\bar{2}0)$ orientated sapphire substrate is first covered at 700 °C by 50 nm of (110) niobium as a chemical buffer, followed by deposition of a 2 nm iron seed layer at 600 °C. The $REFe_2$ compounds are then alternatively grown by co-deposition of iron and yttrium or dysprosium.

The magnetic behavior in the superlattice has been studied by combining superconducting quantum interference device (SQUID) magnetization measurements and XMCD experiments. The former technique enables us to record the net macroscopic magnetization of the whole sample as a function of the applied magnetic field, while the second one has been chosen for the unique capability to isolate the magnetic response of each compound in the superlattice.

In bulk $DyFe_2$, the easy magnetization axis given by the crystal field interaction is $\langle 001 \rangle$ at any temperature [33]. In $DyFe_2$ films, the lattice strains give rise to a supplementary magnetoelastic contribution that drives a change of the easy magnetization axis towards the in-plane $[1\bar{1}0]$ direction when the temperature increases [34]. In YFe_2 films, the easy magnetization axis does not change with temperature and remains close to the $[1\bar{1}1]$ in-plane direction, in agreement with the bulk $\langle 111 \rangle$ easy directions [34]. In the $DyFe_2/YF_2$ superlattices, the magnetometry analysis reveals very similar behaviors for [001] and $[1\bar{1}0]$ directions of applied field below 100 K, while the $[1\bar{1}0]$ direction is obviously easier above 100 K. The results presented in this paper are those collected with the field applied along the $[1\bar{1}0]$ direction.

XMCD experiments were performed on the beamline ID12 of the European Synchrotron Radiation Facility (ESRF). In most of the experiments, the applied magnetic field was parallel to the direction of the incident x-ray beam, at a grazing incidence angle of 8° from in-plane $[1\bar{1}0]$ direction. In this configuration, the signal is proportional to the longitudinal component of the magnetization. Some experiments have also benefited from a specific set up that permits a 90° rotation of both the external field and the sample with respect to the conventional longitudinal geometry; in this transverse configuration, the direction of applied field with respect to the sample is the same as in the longitudinal configuration, but it is rotated by 90° from the direction of incoming x-rays. The XMCD signal is then related to the transverse component of the magnetization.

To record the element-selective hysteresis curves, the energy of the incident x-ray photons was tuned to the maximum of the XMCD signal either at the Dy L_3 edge (2p–5d transitions) or at the Y L_3 edge (2p–4d transitions). The amplitude of the dichroïc signal at each value of the applied field was measured by flipping the helicity of the x-ray beam. The signal was recorded in the total fluorescence detection

mode, which is not sensitive to the external applied magnetic field, at least in the range of interest (+7 to −7 T).

3. Experimental results

3.1. Influence of the cooling field

The superlattice has been field-cooled from 300 to 12 K, for different external magnetic fields H_{fc}, ranging between −7 and +7 T. Similar cooling procedures (same cooling field value) have been used before the measurements of magnetization and XMCD hysteresis loops at 12 K. The results obtained for the different cooling fields are gathered in figure 1: the magnetometry data are reported in the top panel, the XMCD signals measured at the Dy and Y L_3 edges are reported in the middle and bottom panels, respectively. These low temperature behaviors exhibit a small coercivity of less than 1 kOe that is barely detectable on this field scale. Only the first branches recorded from +7 to −7 T are thus shown here for the sake of clarity.

For all cooling field values, the $DyFe_2$ magnetization is not influenced by the field sweeping from +7 to −7 T, as proved by the XMCD signal measured at the Dy edge ($XMCD_{Dy}$) that exhibits very little variation as a function of field. The $DyFe_2$ moments are pinned in this field range, as a result of a large coercivity at low temperature. However, $XMCD_{Dy}$ strongly depends on the cooling field, both in sign and in amplitude, indicating that different magnetic configurations are stabilized during the field-cooling process and are thus frozen at low temperature. Simultaneously, the magnetization reversal in the YFe_2 layers is biased by a field H_Y the amplitude of which reaches 2.5 T for +1 and −1 T cooling fields. Notice that the YFe_2 magnetization is negatively biased since H_Y is negative for positive H_{fc}. The combination of the biased YFe_2 reversal and the pinned $DyFe_2$ magnetization leads to the magnetization curves presented in figure 1 (top curves): they exhibit both a vertical shift due to the pinned $DyFe_2$ magnetization and a horizontal shift due to the biased reversal of unpinned magnetization, i.e. in YFe_2 layers. As a result, the total magnetization measured under +7 T (M_s) and the XMCD signal at the Dy edge ($XMCD_{Dy}$) (filled circles in figures 2(a) and (b), respectively) exhibit similar variations as a function of the cooling field. The horizontal shift of the magnetization curve (H_B) and the bias field for unpinned moments (H_Y) (empty circles in figures 2(a) and (b), respectively) exhibit also the same variations as a function of the cooling field.

More interesting is the clear correlation between the $DyFe_2$ magnetic configuration and the exchange bias effect. Figures 2(a) and (b) attest for this strong interplay: H_B and H_Y exhibit the same dependence on cooling field as M_s, i.e. as the $DyFe_2$ longitudinal magnetic component. This reveals that the exchange bias originates from the quenched $DyFe_2$ magnetization and is directly related to the pinned magnetic configuration. In freezing different magnetic configurations, the different cooling fields freeze different *interface magnetic structures* that are well known to govern exchange bias properties.

Let us, for example, consider the +1 and −1 T cooling field processes that generate approximately the largest M_s (i.e. $XMCD_{Dy}$) and H_B (i.e. H_Y) values. For these applied fields, the magnetic configuration in the superlattice is that of a giant ferrimagnet with antiparallel YFe_2 and $DyFe_2$ net magnetization, as expected from the interface exchange coupling, with the dominant YFe_2 moments parallel to the external field (left column in figure 3) [25]. These +1 and −1 T magnetic fields are not strong enough to break the antiparallel arrangement and drive the $DyFe_2$ magnetization towards the field. In the $DyFe_2$ layers at 12 K, the pinned Dy moments (gray arrows) are thus opposite to the cooling field direction,

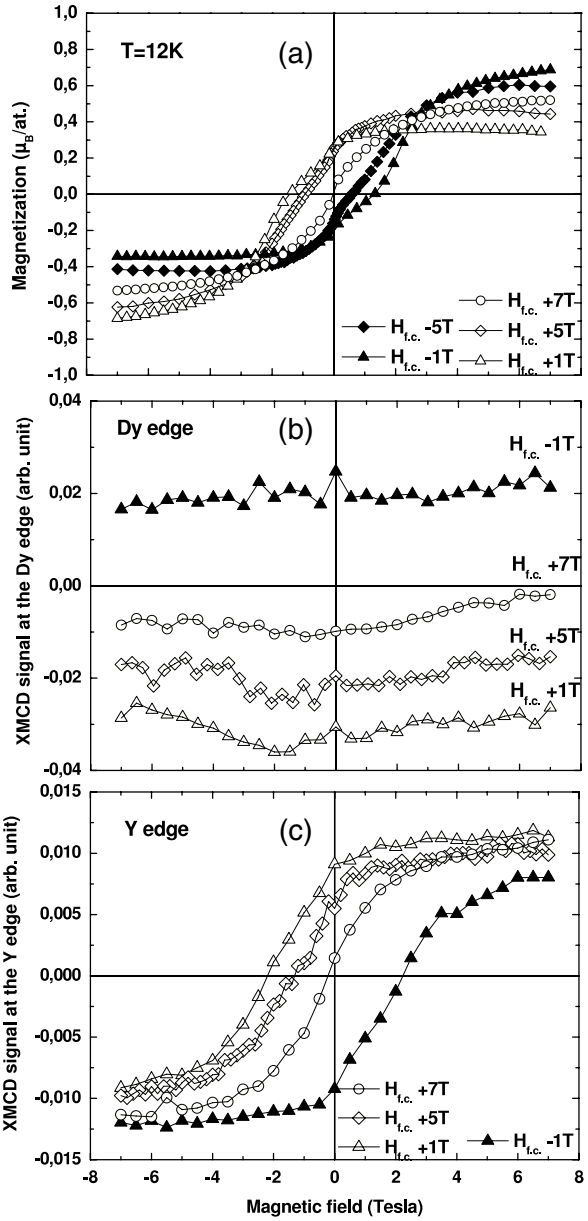

Figure 1. Measurements recorded at 12 K for the superlattice [3 nm $DyFe_2$/12 nm YFe_2]$_{22}$ after field cooling the system from 300 K (the different symbols correspond to different cooling fields H_{fc} given on the figures): (a) magnetization; (b) and (c) XMCD signals recorded at the Dy and Y L_3 absorption edges, respectively. The low temperature coercivity is less than 1 kOe, so barely detectable on this field scale. Only the first branches recorded from +7 to −7 T are thus shown here for the sake of clarity.

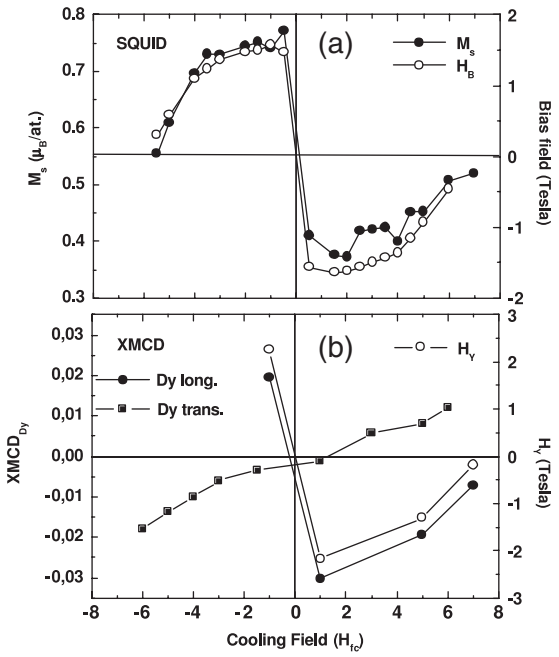

Figure 2. Cooling field dependences for the superlattice [3 nm $DyFe_2$/12 nm YFe_2]$_{22}$ of (a) the saturated magnetization (M_s) and the bias field (H_B) measured by the SQUID, (b) the signal at the Dy edge in the longitudinal configuration ($XMCD_{Dy}$) and the horizontal shift for the Y signal reversal (H_Y) measured by XMCD. The filled squares correspond to the XMCD Dy signal measured in the transverse configuration.

even for a +7 T applied field (right column in figure 3). This results in $XMCD_{Dy} < 0$ for $H_{fc} = +1$ T and $XMCD_{Dy} > 0$ for $H_{fc} = -1$ T. The +7 T field applied at 12 K, however, drives the softer YFe_2 magnetization towards the field. The resulting magnetic interfaces have low energy for $H_{fc} = +1$ T since all Fe moments are parallel; for $H_{fc} = -1$ T, the magnetic configuration for a +7 T applied field implies the development of domain walls parallel to the interfaces (IDW), producing high energy magnetic interfaces. These yield a negative (positive) bias of the YFe_2 reversal for $H_{fc} = +1$ T ($H_{fc} = -1$ T). One can notice that the presence of IDW in the YFe_2 layers for $H_{fc} = -1$ T and $H = +7$ T (symmetrically for $H_{fc} = +1$ T and $H = -7$ T) is visible on the hysteresis loops recorded at the Y L_3 edge (figure 1 bottom): the signals at +7 and −7 T do not have equal magnitudes because of the reduced longitudinal magnetic component in the IDW.

For smaller cooling fields in the −1 T/+1 T range, the magnetic configurations on cooling are probably the same (ferrimagnetic arrangement with YFe_2 magnetization pointing towards the field). For larger cooling fields, the longitudinal component of the $DyFe_2$ magnetization becomes smaller and smaller, as attested by the decreasing $XMCD_{Dy}$ (black dots in figure 2). A second set of experiments using the 90° orientation between the applied field and the x-ray beam has shown that the transverse component of the $DyFe_2$ magnetization simultaneously increases with the amplitude of the cooling field (black squares in figure 2). One can notice that the observation of a non-zero transverse XMCD signal implies that the symmetry is somehow broken; this is probably due to a slight misalignment of the applied field with respect to the [1$\bar{1}$0] direction.

Since the information obtained from the XMCD measurements is an average over the volume probed, the observed reduced longitudinal and increased transverse components in $DyFe_2$ may originate from the tilt of the magnetization with respect to the field direction or from the presence of lateral magnetic domains, pointing either parallel or antiparallel to the field direction.

The coexistence of lateral magnetic domains in $DyFe_2$ can yield the reduction of the bias field if the domains in YFe_2 are larger than in $DyFe_2$ and thus average the bias field over many $DyFe_2$ domains [29]. However, polarized neutron reflectometry measurements (PNR), previously performed on

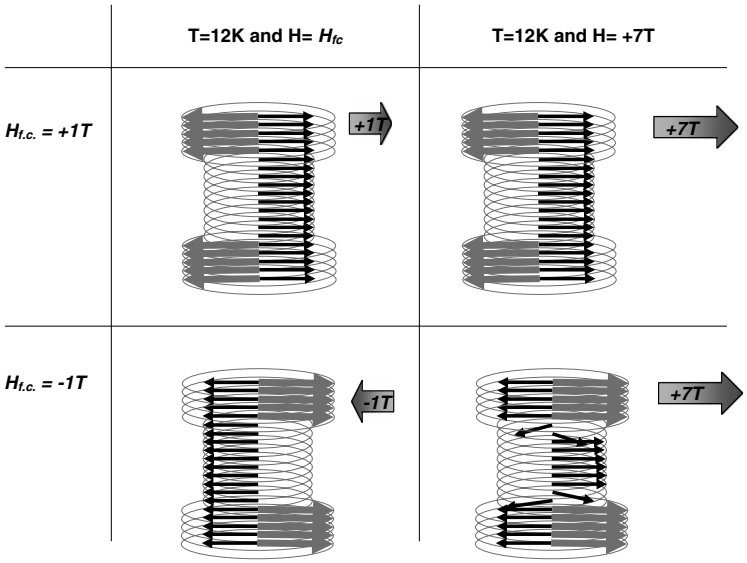

Figure 3. Sketches of the magnetic configurations in the superlattice [3 nm $DyFe_2$/12 nm YFe_2]$_{22}$ at 12 K under H_{fc} (left column) and under +7 T (right column) after field cooling from 300 K (top line: $H_{fc} = +1$ T and bottom line: $H_{fc} = -1$ T). The gray arrows represent Dy moments and the black arrows represent Fe moments.

the same superlattice at 250 K and under +7 T [25], confirm the absence of lateral domains and the rotation of the $DyFe_2$ magnetization away from the negative field direction to reduce the Zeeman energy. This configuration implies the presence of IDW that extend into both the $DyFe_2$ and YFe_2 layers. This rotated configuration in $DyFe_2$, frozen when field cooling the sample down to low temperature, could account for the reduced longitudinal component measured by XMCD. The interface $DyFe_2$ moments would be quenched away from the field direction, which tends to reduce the negative bias field compared, for instance, to the case $H_{fc} = +1$ T where $DyFe_2$ and YFe_2 are homogeneously magnetized and all Fe moments are parallel under +7 T. Other cooling fields in the +1 T/+7 T range are assumed to freeze similar configurations with rotated magnetization. The larger the cooling field, the larger the $DyFe_2$ tilt away from the field, and the larger the angle between the interface $DyFe_2$ quenched moments and the cooling field direction. This turns out to globally increase the energy of magnetic interfaces under +7 T and to reduce the amplitude of the negative bias.

This scenario is consistent with what has been reported for *amorphous* GdFe/TbFe bilayers [28] in which a partial interface domain wall has been shown to freeze in the TbFe hard layer upon field cooling. The observation of a similar phenomenon in this [$DyFe_2$/YFe_2] superlattice that exhibits a *single crystalline* quality is interesting and suggests that its crystalline structure does not play a significant role. PNR analysis [25] leads us to think that frozen magnetic configurations with rotated interfacial spins may also be achieved in this system. Complementary PNR experiments will be performed at 12 K and for different cooling field values to identify more precisely the frozen magnetic configurations achieved in the $DyFe_2$ layers.

Let us finally mention that, in the systems with antiferromagnetic interface coupling, the exchange bias field generally changes from negative to positive as the amplitude of the cooling field is increased [28, 35]. It is negative when the small cooling field stabilizes a low energy magnetic interface. It becomes positive when the cooling field (i.e. the Zeeman contribution) becomes large enough to align the magnetization towards the field and to stabilize high energy magnetic interfaces with IDW. In the present study, the Zeeman gain obtained in aligning homogeneously the $DyFe_2$ magnetization towards the field is small because of the reduced $DyFe_2$ thicknesses in the superlattice. Then, the cooling process under positive magnetic fields (even +7 T) does not enable us to stabilize a positive longitudinal component. The maximum available +7 T cooling field only contributes to reducing the $DyFe_2$ longitudinal component to almost zero, giving rise to a bias field close to zero. In this field range, the bias field thus remains negative, in contrast to what could be expected from the interface exchange energy.

In summary, the exchange bias observed at low temperature is determined by the orientation of the pinned $DyFe_2$ magnetization at the interfaces, which most likely rotates continuously as H_{fc} increases. For any cooling field value, a single loop is measured at 12 K with a bias field continuously varying as M_s, which reflects the different pinned magnetic configurations in the $DyFe_2$ layers and thus at the interfaces.

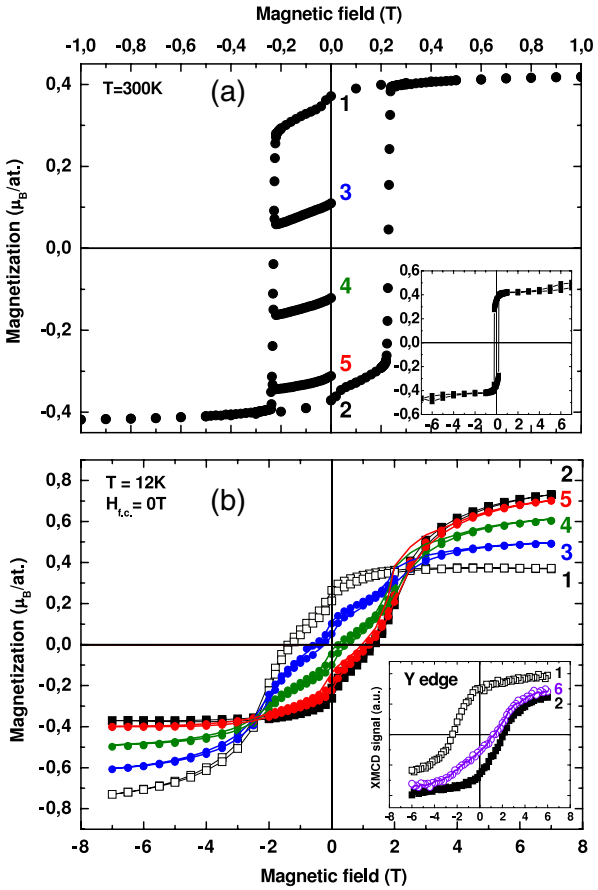

Figure 4. (a) Magnetic preparations of the superlattice [3 nm $DyFe_2$/12 nm YFe_2]$_{22}$ performed at 300 K. The magnetic field is swept from +7 T down to a negative value and back to zero. The labels 1–5 refer to the remanent states achieved after these different field cyclings. The inset presents the hysteresis loop at 300 K in the −7 T/+7 T range. (b) Hysteresis loops measured at 12 K after zero-field cooling from the five remanent states prepared at 300 K (labeled 1–5). The inset presents the XMCD loops recorded at 12 K and at the Y edge for three preparations labeled 1, 2 and 6 (see text). The solid curves are calculated from the superimposition of the experimental curves labeled 1 and 2 (see text for more details).
(This figure is in colour only in the electronic version)

3.2. Influence of the magnetic preparation prior to zero-field cooling

The second part of this study aims to prepare the system in different remanent states at 300 K, in order to freeze (zero-field cooling) different magnetic domain states in the $DyFe_2$ pinning layer at low temperature and to study their influence on the low temperature exchange bias.

At 300 K, the hysteresis loop (inset in figure 4) exhibits three steps that have been identified from previous XMCD analysis [31]. When reducing the magnetic field from +7 T, the $DyFe_2$ magnetization first reverses and the antiparallel configuration between homogeneously magnetized $DyFe_2$ and YFe_2 layers is stabilized by the interface exchange coupling.

In this sample with dominant YFe_2 contribution, YFe_2 magnetization points towards the positive field direction and $DyFe_2$ magnetization is the opposite (arrangement called Ferri+). In a second step, for negative applied fields, the antiparallel arrangement reverses as a block to reduce the Zeeman energy: YFe_2 magnetization points towards the negative field direction and $DyFe_2$ magnetization is opposite (arrangement called Ferri−). Finally, for increasing negative fields, the $DyFe_2$ magnetization tends to align towards the field at the expense of exchange energy at the interfaces (development of IDW).

The idea was to magnetically prepare the system to induce a mixture of domains with Ferri+ and Ferri− arrangements. For this purpose, after applying the maximum +7 T field at 300 K, the field was reduced to a negative value in the field range where the superlattice switches from 100% Ferri+ domains to 100% Ferri− domains, and then increased back to zero (labels 3–5 in figure 4(a)). Two other remanent states (labeled 1 and 2) have been formed to achieve 100% Ferri+ domains (field reduced from 7 to 0 T) and 100% Ferri− domains (field reduced from +7 T to −0.3 T and back to 0 T). The proportion f_i of Ferri− domains formed by preparation i can be deduced from M_i, the magnetization value at 0 T at the end of the field cycling: $f_i = (M_i - M_1)/(M_2 - M_1)$. We obtain $f_1 = 0$, $f_2 = 1$, $f_3 = 0.35$, $f_4 = 0.67$ and $f_5 = 0.92$.

The superlattice is then cooled down to 12 K under zero field and hysteresis loops are measured (figure 4(b)). XMCD experiments have also been performed after similar magnetic preparations (labeled 1, 2 and 6). The proportion f_6 of Ferri− domains formed by preparation 6 was deduced from the XMCD value at 0 T at the end of the field cycling at 300 K ($f_6 = 0.73$). The half loops recorded at 12 K at the Y edge are presented as an inset in figure 4(b). As previously, the low temperature magnetization loops exhibit strong vertical and horizontal shifts, related to pinned magnetization and exchange bias phenomena, respectively. They strongly depend on the 300 K initial remanent state, which proves that different magnetic arrangements have been frozen in the $DyFe_2$ layers *despite the same zero-field cooling*. An interesting point concerns the shapes of the loops. Those obtained after preparations 1 and 2 are very similar to those measured after +1 and −1 T field-cooling processes (figure 1); after preparations 3, 4 and 5, the shapes of the loops are significantly different and appear as linear combinations of 1 and 2 loops, i.e. of the two loops that are shifted by the maximum bias field toward negative and positive directions, respectively. The solid curves in figure 4(b) (labels 3–5) are calculated using the following formula: $f_i M_2(H) + (1 - f_i)M_1(H)$, where $M_1(H)$ and $M_2(H)$ are the low temperature loops recorded after the magnetic preparations 1 and 2, respectively. The solid curve in the inset is also a linear combination of $XMCD_1(H)$ and $XMCD_2(H)$ using $f_6 = 0.73$. The very good agreement between the calculated and experimental data signifies that (i) the domains formed at 300 K in $DyFe_2$ are unchanged after cooling (ii) the part of the sample which is biased positively (negatively) corresponds to the domains with $DyFe_2$ magnetization pointing along the positive (negative) field direction. In both Ferri+ and Ferri− arrangements, the $DyFe_2$ layers are magnetized homogeneously in the depth of the sample, respectively opposite and towards the positive field direction (figure 3). These give rise to maximum negative and positive bias values, respectively.

The superlattice thus behaves as if it consisted of two independent subsystems exchange biased in an opposite manner. This result is in agreement with the presence of large, independent domains with opposite spin orientation in the $DyFe_2$ pinning layer [29, 30]. To give rise to their own bias field, these domains must be larger than the characteristic magnetic length scale in the YFe_2 layers.

4. Conclusion

In summary, a large exchange bias is observed at low temperature in the exchange-coupled [3 nm $DyFe_2$/12 nm YFe_2]$_{22}$ superlattice. This effect is attributed to the presence of pinned magnetization (in $DyFe_2$ layers) that biases the reversal of the unpinned component (YFe_2). As a consequence, the magnetic preparation of the system is determinant in tailoring the low temperature exchange bias behavior, since it is possible to freeze different magnetic configurations in $DyFe_2$ layers, especially at the interfaces with YFe_2.

Field cooling the sample yields a single hysteresis loop and the bias field varies continuously with the amplitude of the cooling field. For increasing cooling field, the $DyFe_2$ magnetization is probably more and more rotated from the cooling field direction, giving rise to IDW that partly extend in the $DyFe_2$ layers and that are quenched at low temperature. The dependence of bias field on the cooling field thus reflects the orientation of the interface pinned $DyFe_2$ moments.

When the superlattice is zero-field-cooled from a specific remanent state with large lateral domains in the pinning $DyFe_2$ layers (partial demagnetization), the low temperature loop results from the superimposition of positively and negatively biased loops whose relative proportions reflect the domain populations.

These exchange-coupled $DyFe_2/YFe_2$ superlattices combining hard and soft ferrimagnets therefore make an interesting system to focus on exchange bias phenomena and especially to investigate the role of the magnetic configuration in the pinning layer. This study illustrates how the exchange bias is governed by the pinning layer magnetization at the interfaces and shows the role of large lateral domains in the pinning layer.

Acknowledgments

The authors would like to thank the technical staff of the Laboratoire de Physique des Matériaux (UMR 7556) for their constant help and especially Danielle Pierre for the fabrication of the samples.

References

[1] Kneller E F 1991 *IEEE Trans. Magn.* **27** 3588
[2] Nogués J and Schuller I K 1999 *J. Magn. Magn. Mater.* **192** 203
[3] Berkowitz A E and Takano K 1999 *J. Magn. Magn. Mater.* **200** 552

[4] Meiklejohn W H and Bean C P 1957 *Phys. Rev.* **102** 1413
[5] Kiwi M 2001 *J. Magn. Magn. Mater.* **234** 584
[6] Stamps R L 2000 *J. Phys. D: Appl. Phys.* **33** R247
[7] Ohldag H, Regan T J, Stöhr J, Scholl A, Nolting F, Lüning J, Stamm C, Anders S and White R L 2001 *Phys. Rev. Lett.* **87** 247201
[8] Ohldag H, Scholl A, Nolting F, Arenholz E, Maat S, Young A T, Carey M and Stöhr J 2003 *Phys. Rev. Lett.* **91** 017203
[9] Hoffmann A, Seo J W, Fitzsimmons M R, Siegwart H, Fompeyrine J, Locquet J P, Dura J A and Majkrzak C F 2002 *Phys. Rev.* B **66** 220406(R)
[10] Roy S, Fitzsimmons M R, Park S, Dorn M, Petracic O, Roshchin I V, Li Z-P, Battle X, Morales R, Misra A, Zhang X, Chesnel K, Kortright J B, Sinha S K and Schuller I K 2005 *Phys. Rev. Lett.* **95** 047201
[11] Fitzsimmons M R, Kirby B J, Roy S, Li Z-P, Roshchin I V, Sinha S K and Schuller I K 2007 *Phys. Rev.* B **75** 214412
[12] Brück S, Schütz G, Goering E, Ji X and Krishnan K M 2008 *Phys. Rev. Lett.* **101** 126402
[13] Ball A R, Leenaers A J G, van der Zaag P J, Shaw K A, Singer B, Lind D M, Frederikze H and Rekveldt M Th 1996 *Appl. Phys. Lett.* **69** 583
[14] te Velthuis S G E, Felcher G P, Jiang J S, Inomata A, Nelson C S, Berger A and Bader S D 1999 *Appl. Phys. Lett.* **75** 4174
[15] Coey J M D and Skomski R 1993 *Phys. Scr.* T **49** 315
[16] Gordeev S N, Beaujour J M L, Bowden G J, Rainford B D, de Groot P A J, Ward R C C, Wells M R and Jansen A G M 2001 *Phys. Rev. Lett.* **87** 186808
[17] Dumesnil K, Dutheil M, Dufour C and Mangin Ph 2000 *Phys. Rev.* B **62** 1136
[18] Fullerton E E, Jiang J S, Grimsditch M, Sowers C H and Bader S D 1998 *Phys. Rev.* B **58** 12193
[19] Sawicki M, Bowden G J, de Groot P A J, Rainford B D, Beaujour J M L, Ward R C C and Wells M R 2000 *Phys. Rev.* B **62** 5817
[20] Hellwig O, Kortright J B, Takano K and Fullerton E E 2000 *Phys. Rev.* B **62** 11694
[21] Radu F, Etzkorn M, Siebrecht R, Schmitte T, Westerholt K and Zabel H 2003 *Phys. Rev.* B **67** 134409
[22] Mangin S, Marchal G and Barbara B 1999 *Phys. Rev. Lett.* **82** 4336
[23] Zeng H, Li J, Lu J P, Wang Z L and Sun S 2002 *Nature* **420** 395
[24] Ritter C 1989 *J. Phys.: Condens. Matter* **1** 2765
[25] Fitzsimmons M R, Park S, Dumesnil K, Dufour C, Pynn R, Borchers J A, Rhyne J J and Mangin Ph 2006 *Phys. Rev.* B **73** 134413
[26] Nogués J, Leighton C and Schuller I K 2000 *Phys. Rev.* B **61** 1315
[27] Kirk T L, Hellwig O and Fullerton E E 2002 *Phys. Rev.* B **65** 224426
[28] Henry Y, Mangin S, Hauet T and Montaigne F 2006 *Phys. Rev.* B **73** 134420
[29] Roshchin I V, Petracic O, Morales R, Li Z P, Battle X and Schuller I K 2005 *Europhys. Lett.* **71** 297
[30] Mangin S, Hauet T, Henry Y, Montaigne F and Fullerton E E 2006 *Phys. Rev.* B **74** 024414
[31] Dumesnil K, Dufour C, Mangin Ph, Rogalev A and Wilhelm F 2005 *J. Phys.: Condens. Matter* **17** 21
[32] Oderno V, Dufour C, Bauer Ph, Dumesnil K, Mangin Ph and Marchal G 1996 *J. Cryst. Growth* **165** 175
[33] Bowden G J, Bunbury D S P, Guimaraes A P and Snyder R E 1968 *J. Phys. C: Solid State Phys.* **1** 1376
[34] Mougin A, Dufour C, Dumesnil K and Mangin Ph 2000 *Phys. Rev.* B **62** 9517
[35] Nogués J, Lederman D, Moran T J and Schuller I K 1996 *Phys. Rev. Lett.* **76** 4624